**Atmospheric
Chemistry
and Physics**

Primary and secondary contributions to aerosol light scattering and absorption in Mexico City during the MILAGRO 2006 campaign

G. Paredes-Miranda[1], W. P. Arnott[1], J. L. Jimenez[2], A. C. Aiken[2], J. S. Gaffney[3], and N. A. Marley[4]

[1]Department of Physics, University of Nevada Reno, and the Desert Research Institute, Reno, NV, USA
[2]Deptartment of Chemistry and Biochemistry and CIRES University of Colorado, Boulder, CO, USA
[3]Department of Chemistry, University of Arkansas, Little Rock, AK, USA
[4]Graduate Institute of Technology, University of Arkansas, Little Rock, AK, USA

Abstract. A photoacoustic spectrometer, a nephelometer, an aethalometer, and an aerosol mass spectrometer were used to measure at ground level real-time aerosol light absorption, scattering, and chemistry at an urban site located in North East Mexico City (Instituto Mexicano del Petroleo, Mexican Petroleum Institute, denoted by IMP), as part of the Megacity Impact on Regional and Global Environments field experiment, MILAGRO, in March 2006. Photoacoustic and reciprocal nephelometer measurements at 532 nm accomplished with a single instrument compare favorably with conventional measurements made with an aethalometer and a TSI nephelometer. The diurnally averaged single scattering albedo at 532 nm was found to vary from 0.60 to 0.85 with the peak value at midday and the minimum value at 07:00 a.m. local time, indicating that the Mexico City plume is likely to have a net warming effect on local climate. The peak value is associated with strong photochemical generation of secondary aerosol. It is estimated that the photochemical production of secondary aerosol (inorganic and organic) is approximately 75% of the aerosol mass concentration and light scattering in association with the peak single scattering albedo. A strong correlation of aerosol scattering at 532 nm and total aerosol mass concentration was found, and an average mass scattering efficiency factor of 3.8 m^2/g was determined. Comparisons of photoacoustic and aethalometer light absorption with oxygenated organic aerosol concentration (OOA) indicate a very small systematic bias of the filter based measurement associated with OOA and the peak aerosol single scattering albedo.

Correspondence to: G. Paredes-Miranda
(gparedes@physics.unr.edu)

1 Introduction

About 20% of the Mexican population lives in the Mexico City metropolitan area (MCMA) in a megacity environment with approximately 23 million occupying less than 1% of the Mexican territory according to the 2005 census. Mexico City consists of 125 town councils, and 16 delegations and consists of 23 842 km^2 of territory, although a large part of this area includes mountains and rural zones without urbanization (http://www.inegi.gob.mx). This megacity has developed with a significant dependence on its transportation system. Most of the air pollution in Mexico City comes from the combustion of fossil fuels (gasoline and diesel) in motor vehicles. Approximately 75% of the 4 million tons of pollutants generated yearly in the metropolitan area comes from motor vehicles according to the Mexican emissions inventory (Mar et al., 2001). Biomass burning (BB) can also be a relevant pollution source during the dry season (March–June), especially for particulate matter (PM) (DeCarlo et al., 2008; Molina et al., 2007; Yokelson et al., 2007), although the importance is significantly higher aloft and in the outflow than on the ground inside the city, and BB impacts on the ground were highly variable in time during MILAGRO (Aiken et al., 2009; Stone et al., 2008).

The seasonal variation of the daily maximum vertical component of solar irradiance at the top of the atmosphere above Mexico City varies between 1040 W/m^2 at the winter minimum and 1327 W/m^2 at the summer maximum due to its subtropical location at latitude 19 degrees north. Solar radiation and the relatively high elevation of Mexico City give rise to strong ventilation of the city where residence times for pollutants is on the order of 7 h and the atmospheric boundary layer height can vary from 2 km to 4 km above ground level

(de Foy et al., 2006). Stagnant conditions associated with low wind speeds can produce locally high concentrations of pollutants, depending on the wind direction. The topography surrounding the MCMA basin gives rise to characteristic flow patterns on different days with flow associated with convergence and pollution buildup in the south of MCMA, flow that drains to the northeast, and "cold surges" associated with low atmospheric boundary layer heights where cold air from the north drains through the Chalco passage in the southeast of the MCMA (de Foy et al., 2006). These flow patterns give rise to pollutant concentrations that can vary markedly from day to day; however, it is the purpose of this paper to seek an understanding of the average diurnal behavior of aerosol concentrations and optical properties during the month of March, 2006.

Aerosol light scattering and absorption have considerable radiative impacts that can lead to cooling or heating, respectively. A comparison of the intensity of global radiation in Mexico City with that over a nearby rural area for the same time was performed to estimate attenuation of the solar beam by the smog layer (Jauregui and Luyando, 1999). These authors found that reduction of total solar incoming radiation is on the order of 21–22% on non-cloudy days during both the dry and the rainy seasons. Inorganic and organic aerosols tend to strongly scatter and backscatter visible solar radiation, and are associated with a cooling effect on climate (Charlson et al., 1992; Haywood and Ramaswamy, 1998). Black carbon aerosols strongly absorb radiation from the near infrared through the ultraviolet and tend to have a warming effect on climate (Andreae, 2001; Haywood and Ramaswamy, 1998; Jacobson, 2001). Black carbon has long been associated with "elemental carbon", though other carbonaceous species absorb light as well, particularly at UV wavelengths (Andreae and Gelencsér, 2006; Kirchstetter et al., 2004). A more apt name for aerosol light absorption by organic carbon species is brown carbon because of their selective absorption at shorter wavelengths (Sun et al., 2007).

Filter-based measurement of aerosol light absorption by organic species is complicated because they can exist in the liquid state and wet the filter material (Subramanian et al., 2007). Calibration efforts for the filter-based measurement of aerosol light absorption have only considered aerosol as solids rather than as liquids (Arnott et al., 2005; Bond et al., 1999; Virkkula et al., 2007; Weingartner et al., 2003). A recent review of aerosol light absorption issues is available (Bond and Bergstrom, 2006). Recent measurements in Houston, TX, USA indicate a systematic positive bias of the filter-based instrument, the particle soot absorption photometer in the presence of high secondary organic aerosol concentration (Lack et al., 2008).

Analyses of aerosol measurements during the MCMA-2003 field campaign (Molina et al., 2007; Salcedo et al., 2006; Volkamer et al., 2006, 2007) show that the submicron aerosol mass in Mexico City during the spring is dominated by secondary species (nitrate, sulfate, ammonium, chloride,

and secondary organic aerosol or SOA) with the main primary species being primary organic aerosol or POA, black carbon, and crustal material. Salcedo et al. (2006) described the rapid formation of ammonium nitrate in the local Mexico City atmosphere, while ammonium sulfate seemed to be formed more slowly and over larger regional scales. Ammonium chloride was also observed in small concentrations, but its diurnal cycle seemed to reflect primarily its semivolatile character. Volkamer et al. (2006) showed that formation of SOA was rapid and exceeded the predictions of current models by almost an order of magnitude.

This paper reports diurnally averaged aerosol light scattering and absorption measurements made using photoacoustic, nephelometer, and aethalometer instruments during the MILAGRO campaign in March, 2006. Aerosol mass spectrometer measurements of the submicron speciated organics and inorganics were also diurnally averaged. These measurements are combined to show the radiative and chemical impacts of primary and secondary aerosols in the MCMA. The diurnal variation of aerosol chemistry and optics is used to estimate the contributions of secondary aerosol formation to particulate mass and light scattering.

2 Experimental

2.1 Sites

The MILAGRO (Megacity Initiative: Local and Global Research Observations) campaign took place in Mexico City in the MCMA during the month of March 2006 (http://www.eol.ucar.edu/projects/milagro). The campaign was carried out to better understand the local, regional and global impact of pollutants generated in megacities, considering health effects and visibility issues as well as climate impacts. The MILAGRO field experiment involved more than 400 researchers from over 120 institutions in the USA, Mexico, and several other countries. The campaign involved coordinated aircraft and ground-based measurements supported by extensive modeling and satellite observations (de Almeida Castanho et al., 2007). Three main sites were strategically chosen to characterize the transport and transformation of the pollutants carried from the urban area of the city, and to take measurements on the ground; one in the urban area of Mexico City designated T0 located in Northeast Mexico City at the Instituto Mexicano del Petroleo (IMP), and the other two, T1 and T2 were located, respectively at urban and rural locations with approximated 32 km and 63 km north of IMP (Querol et al., 2008).

2.2 Measurement methods

Aerosol light scattering and absorption instruments were calibrated, installed, and operated at the T0 site. Aerosol light absorption was measured by the photoacoustic spectrometer

(PAS) method. The PAS provides a fundamental measurement of aerosol light absorption based on use of a calibrated microphone to measure the sound produced when light absorbing aerosol in the acoustical resonator are heated by laser light absorption and transfer that heat to the surrounding air (Arnott et al., 1999). The PAS instrument accuracy has been evaluated and confirmed using both gaseous light absorption by NO_2 (Arnott et al., 2000) and through the use of the subtraction of aerosol light scattering from aerosol extinction for laboratory generated external mixtures of kerosene soot and ammonium sulfate (Sheridan et al., 2005). The PAS used at IMP was operated at 532 nm, and conveniently allowed for characterization of gaseous (i.e. NO_2) absorption at this wavelength as well when a particle filter was used on the inlet. Simultaneous light scattering measurements are accomplished within the PAS by use of an optical sensor configured to operate as a reciprocal nephelometer (Rahmah et al., 2006). The reciprocal nephelometer measurements of scattering coefficient have a systematic relative uncertainty of 15%, and the photoacoustic absorption coefficient measurements have a 5% relative uncertainty (Lewis et al., 2008) associated with systematic errors noted during repeated calibrations. Independent light scattering measurements were also obtained at the site by using a three-wavelength TSI Model 3550 nephelometer at 450 nm, 550 nm, and 700 nm (Anderson et al. 1996).

Aerosol light absorption data were also obtained with a filter-based method, the 7-wavelength aethalometer (370, 470, 520, 590, 660, 880 and 950 nm). The use of the aethalometer to estimate aerosol light absorption in urban locations has been discussed previously (Arnott et al., 2005). In brief, the aethalometer measurement uses light transmission measurements through an aerosol laden quartz fiber filter. The change of light transmission with time is first used to obtain the aerosol absorption optical depth as affected by multiple scattering enhancements by the fiber media. Then the instrument algorithm computes a black carbon mass concentration (BC) with use of the measured flow rate, sample time, and an assumed filter multiple-scattering-enhanced mass-absorption-efficiency that is about a factor of two larger than would be appropriate for the same particles dispersed in air as an aerosol. The factor of two comes about because it is equally possible for light to be going through the filter in either direction as a consequence of multiple scattering so that for a clean filter, particles deposited on the filter have two chances for absorbing a given photon. Finally, an empirically derived mass absorption efficiency of 8.8 m^2/g was determined, using a PAS and an aethalometer in urban Las Vegas, Nevada, USA, to be relevant for converting the aethalometer BC measurements at 520 nm to aerosol light absorption at 532 nm to correct for the filter enhancement of absorption (Arnott et al., 2005).

Real time chemical characterization of the PM$_1$ aerosol composition was obtained with a High-Resolution Aerosol Mass Spectrometer (AMS) (Canagaratna et al., 2007; De-Carlo et al., 2006; Jimenez et al., 2003). The AMS provides mass concentration of non-refractory inorganic (nitrate, ammonium, sulfate, and chloride) and organic aerosol (OA). The organic aerosol can be apportioned among different components using factor analysis techniques on the AMS spectra (Zhang et al., 2005, 2007). For this study the Positive Matrix Factorization (PMF) method was applied on the unit-resolution AMS spectra (Paatero and Tapper, 1994; Ulbrich et al., 2008) which allowed the quantification of hydrocarbon-like OA (HOA), oxygenated organic aerosol (OOA) as a surrogate for secondary organic aerosol (SOA), and biomass-burning OA (BBOA). PMF of the high-resolution spectra, which is in progress and will be presented in a future publication, shows similar results with more detail on the apportionment (Aiken et al., 2008; Aiken et al., 2009). The mass concentration measurements obtained with the AMS have an uncertainty of about 20% due to the uncertainty of particle collection efficiency (Huffman et al., 2005; Salcedo et al., 2006).

Aerosol optics measurements were accomplished under dry conditions owing to the generally low relative humidity (below 50%) observed in the instruments. In addition, all measurements are reported at Central Standard Time (CST), the local time in Mexico City. All measurements are reported at ambient pressure and temperature. To convert concentrations to standard temperature and pressure conditions (STP, 1 atm and 273 K) the values reported here should be multiplied by approximately 1.42. It was estimated that the sampling inlets on the instrumentation resulted in an effective size cut of PM$_1$ (i.e. one micron). The fraction of the PM$_{2.5}$ mass between PM$_1$ and PM$_{2.5}$ in Mexico City is typically small (Salcedo et al., 2006; Querol et al., 2008), so slight differences in the detailed size cuts of the different instruments should only lead to small differences on the aerosols sampled.

3 Results and discussion

Comparisons of PAS with aethalometer absorption and TSI nephelometer scattering data are presented in Figs. 1 and 2. The data demonstrate good agreement of the PAS measurements for scattering and absorption with these other commonly employed methods. These comparisons are consistent with the accuracy demonstrated in previous comparisons of light absorption and scattering using similar instrumentation (Arnott et al., 2005; Rahmah et al., 2006).

Significant diurnal variations of aerosol light absorption and scattering were observed and are attributed in part due to changes in the meteorology in the Mexico City Basin and the sources of aerosols impacting the IMP site (see Fig. 3). On the diurnal average, the aerosol light absorption and scattering coefficients were found to vary between 20 and 80 Mm^{-1} and between 60 and 170 Mm^{-1}, respectively. Gaseous light absorption at 532 nm, likely associated
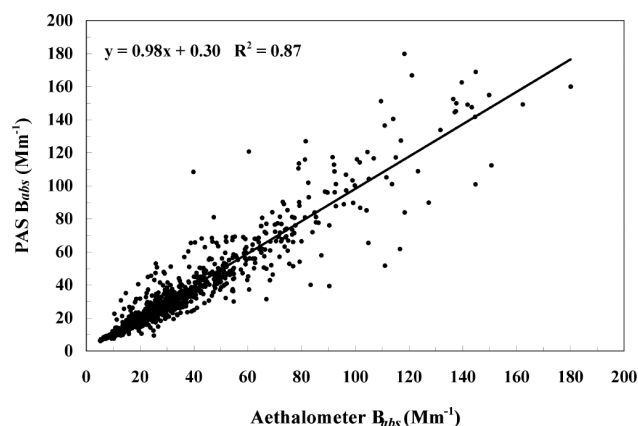
Fig. 1. Light absorption comparison of PAS with Aethalometer at 532 nm and 520 nm at the IMP site. Each point represents a 30 min average.
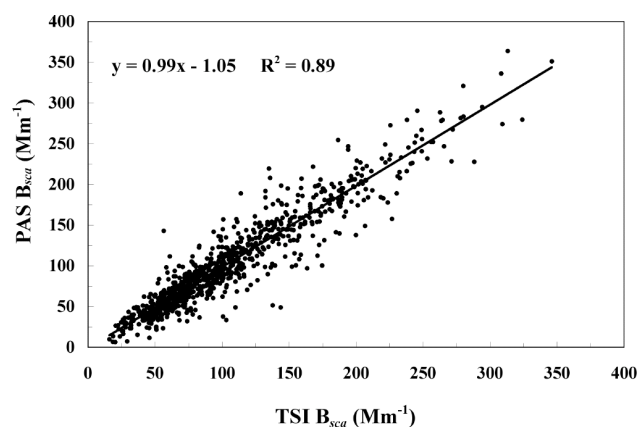

Fig. 2. Light scattering comparison of PAS with TSI at 532 nm and 550 nm at the IMP site. Each point is a 30 min average.

Fig. 3. Diurnal variation of aerosol light absorption, scattering, and extinction at 532 nm.

Fig. 4. Diurnal single scattering albedo (dark curve and circles) varies between 0.6 and 0.85 at 532 nm, and begins to flatten out around 10 as extinction (shaded curve and triangles) diminishes. Nighttime is the shaded region.

with NO_2, was less than $20\,Mm^{-1}$ on average. The peak in aerosol light scattering occurs several hours later in the day than the absorption peak because of aerosol light scattering contributions from photochemically-generated secondary aerosol mass and perhaps due to diurnal changes in the primary aerosol sources. Note that the aerosol concentration at night above the boundary layer is typically small (e.g. OOA background levels are ≈ 2–$3\,\mu g\,m^{-3}$ under ambient conditions (Herndon et al., 2008)) and thus the air which is being mixed down with the urban air during the boundary layer rise in the morning does not greatly perturb the observations presented here. The peak in aerosol light absorption is likely to coincide with the time of early morning traffic rush hour under low atmospheric boundary layer height before sunrise. Previous diurnally averaged aethalometer measurements at the Centro Nacional de Investigación y Capacitación Ambiental (CENICA) supersite located southeast of the T0 site in Mexico City in April 2003 showed an equivalent aerosol
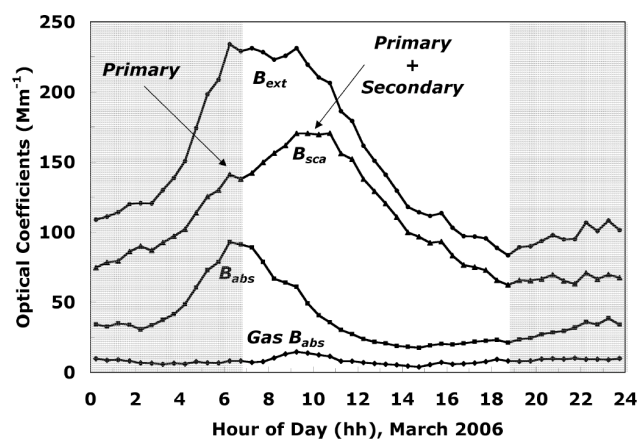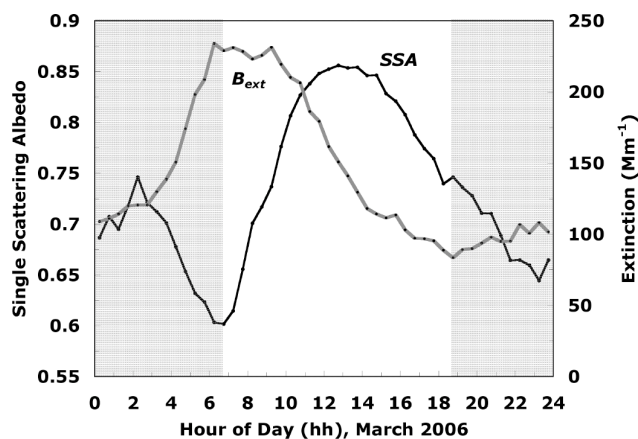
light absorption at 532 nm ranging from 22 to $66\,Mm^{-1}$, with a similar timing of the peak value when the CENICA measurements are converted from Central Daylight Savings Time to Central Standard Time (Salcedo et al., 2006). The 30 min averaged maximum aerosol extinction coefficient on an average day is about $230\,Mm^{-1}$. It is associated with both primary emissions and secondary formation and extends from around 06:00 a.m. until 10:00 a.m.

The aerosol single scattering albedo (SSA) at 532 nm was calculated from the scattering and extinction measurements shown in Fig. 3. The SSA absolute uncertainty varies somewhat during the day, but it is typically about 0.03, just as in McComiskey et al. (2008). Significant diurnal variation of the aerosol single scattering albedo (SSA) was observed as shown in Fig. 4. Daily averaged minimum SSA values are 0.60 coincident with absorption peaks in the early morning. By noon local time the maximum averaged SSA value
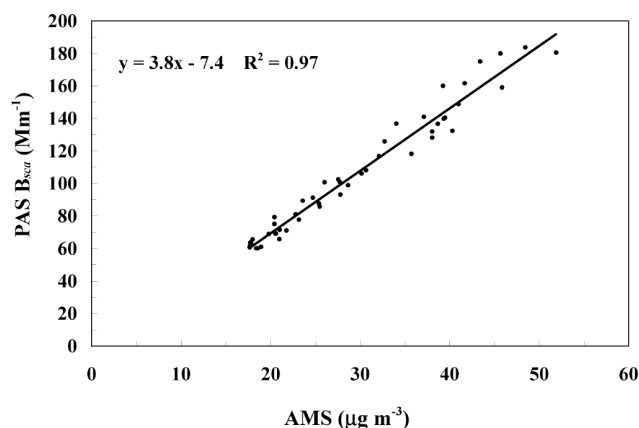
Fig. 5. Correlation of aerosol light scattering at 532 nm with total submicron aerosol mass. The mass scattering efficiency is 3.8 m²/g. Data are from the diurnal average shown in Fig. 6.

Fig. 6. Diurnal variation of aerosol chemistry and optics.

of 0.85 is observed, coincident with boundary layer height development and ventilation that dilute primary emissions of light absorbing aerosol. Photochemically generated secondary particle mass produces a rapid increase in SSA as soon as the sun rises to a peak around noon. The diurnally averaged single scattering albedo is roughly the same for approximately 3 h centered on local 14:00 as boundary layer dilution is balanced by secondary aerosol formation and continuing primary emissions of scattering and absorbing aerosol. Direct measurements of aerosol single scattering albedo is especially important because of its strong impact on direct aerosol radiative forcing (McComiskey et al., 2008). Aerosol single scattering albedo values are strongly dependent on primary sources and secondary atmospheric chemistry, as well as other parameters such as the combustion intensity and flaming and smoldering fraction of biomass burning events. For example, the flaming stage of bushes such as sage produces smoke with a SSA of around 0.3 at 532 nm (Lewis et al., 2008), very similar to the value found for kerosene and diesel soot (Arnott et al., 2000; Sheridan et al., 2005), while combustion of pines and duffs results in SSAs between 0.9 and 1.0 (Lewis et al., 2008). Aerosol mixing state and chemistry impact optical properties.

Previous measurements of total $PM_{2.5}$ in Mexico City, 2003, have been shown to agree well with the sum of aerosol species from the AMS plus refractory BC and soil (Salcedo et al., 2006), and most of the aerosol mass in MCMA is likely in internally mixed particles by the afternoon (Johnson et al., 2005; Salcedo et al., 2007). In the current study, total aerosol scattering at 532 nm correlates well with total PM_1 aerosol mass as obtained from the AMS plus refractory BC obtained from the photoacoustic measurements of light absorption and use of a mass absorption efficiency factor of 8.8 m²/gram, as shown in Fig. 5. The mass scattering efficiency of 3.8 m²/g was determined from the linear regression, which is the same as the value found by DeCarlo et al. (2008) with measure-
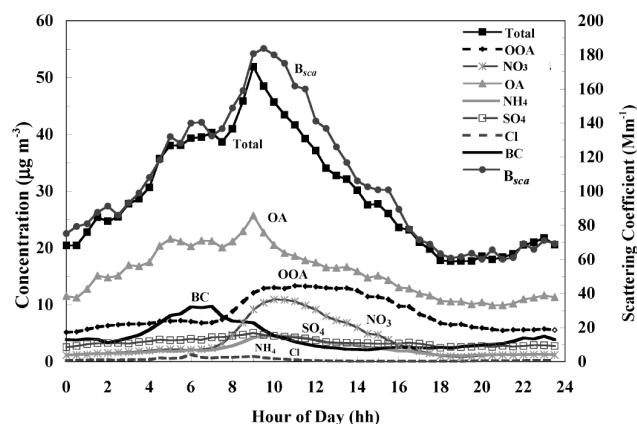
ments around the Mexico City region from the NCAR C-130 aircraft. For comparison, other mass scattering efficiency factors at 550 nm found in megacity environments include values of 4.9 m²/g in India, and 3.4 m²/g in Beijing (Bergin et al., 2001; Mayol-Bracero et al., 2002). The linear regression shown in Fig. 5 shows a small systematic variation of the aerosol mass scattering efficiency that will be discussed later.

Figure 6 displays the diurnal variation of PM_1 along with its components, and the aerosol scattering coefficient at 532 nm. Figure 6 illustrates the close relationship of PM_1 and aerosol light scattering throughout the average day with a slight tendency of increased aerosol mass scattering efficiency during daylight hours. The PM_1 used here is a sum of BC, the inorganic species, and the total organic aerosol mass (OA). A small negative bias is associated with the omission of crustal material, which however usually only constitutes a few percent of the PM_1 aerosol (Salcedo et al., 2006). BC was estimated by dividing the photoacoustic light absorption measurements at 532 nm by a mass absorption efficiency factor of 8.8 m²/g. The oxygenated organic aerosol (OOA), NH_4, and NO_3, all have a diurnal trend that is distinctly different from the BC diurnal trend, strongly suggesting that a substantial fraction of the OOA, NH_4, and NO_3 are produced by same-day secondary photochemical processes in addition to a fraction that appears to arise from carryover from the previous day and/or from regional background. It should be noted that the biomass burning organic aerosol (BBOA) and hydrocarbon-like organic aerosol (HOA) (not shown) generally follow a diurnal trend very similar to that of BC (Aiken et al., 2009). In summary, certain species and properties such as BC and aerosol light absorption, HOA, and BBOA tend to follow diurnal emission patterns and atmospheric boundary layer dynamics, while others such as aerosol light scattering, PM_1, OOA, NH_4, and NO_3 have a strong diurnal component. We next develop an estimate of the fraction of aerosol
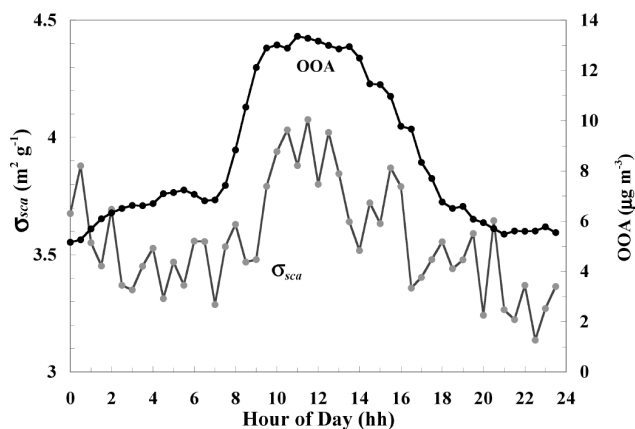
Fig. 7. Mass scattering efficiency as a function of time of day, and the OOA.
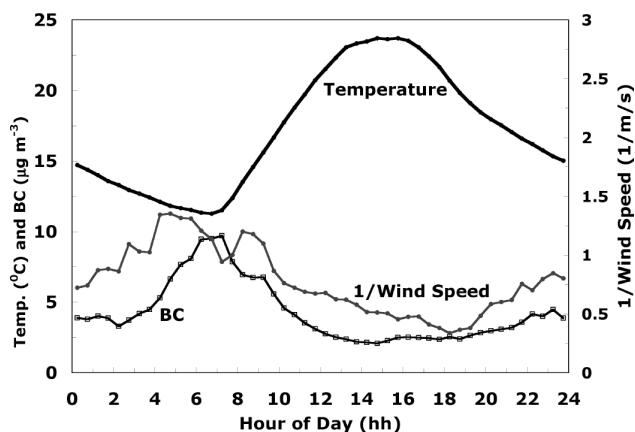

Fig. 8. Average diurnal variation of the air temperature, black carbon mass concentration (BC), and reciprocal wind speed. Reciprocal wind speed is proportional to air parcel residence time in the city and is a measure of stagnation.

Fig. 9. BC and PM$_1$ mass concentration scaled to a constant planetary boundary layer. The peak PM$_1$ lags the peak solar irradiance at the top of the atmosphere by two hours.

light scattering and mass concentration with a diurnal trend suggestive of same-day secondary photochemical processes.

Figure 7 shows the diurnal variation of the mass scattering efficiency and OOA. The peak value of mass scattering efficiency, 4.1 m^2/g, is observed to occur at midday coincident with the peak OOA concentration, while the lowest values ~3.3 m^2/g occur in the late evening and early morning, consistent with the increased fraction of smaller primary particles. Both aerosol size and composition may affect the mass scattering efficiency.

The diurnal variation of some of the planetary boundary layer (PBL) characteristics, and BC are shown in Fig. 8. The reciprocal of wind speed is directly proportional to the residence time of air parcels in the city, and is a measure of stagnation. BC peaks at sunrise when the air temperature is lowest and the air is most stagnant. By 02:00 p.m. the air temperature is maximum, the air is least stagnant, and
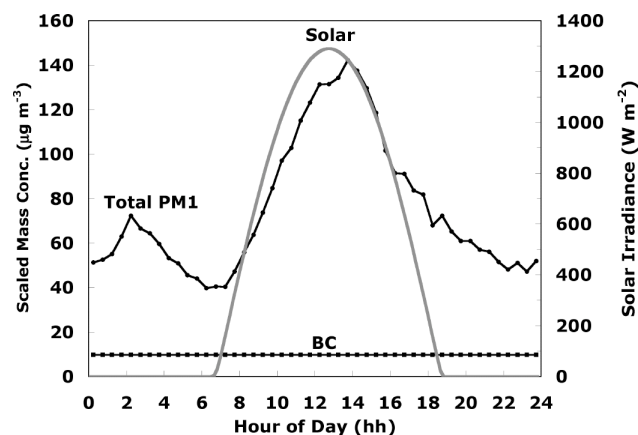
black carbon concentration is also lowest. If BC were emitted at a constant rate through out the day, and the deposition rate is constant, then BC would be a measure of the dilution during the day as the PBL develops. Figure 9 shows the PM$_1$ and BC concentration scaled so that BC is at its peak value all day long. The purpose of this figure is to estimate what the PM$_1$ concentration would be during the day if only secondary aerosol generation mechanisms were active, but the PBL was otherwise constant at a fixed height. The peak normalized-PM$_1$ occurs a few hours after the peak solar irradiance during the day due to generation of aerosol of mass by secondary photochemical processes. A second peak occurs in the early morning hours possibly as a consequence of the diminishing air temperature that favors condensation of vapors on existing particles. The effect of biomass burning POA is approximately accounted for by the normalization to BC, since this component has a similar diurnal cycle as BC (Aiken et al., 2009).

In estimating the contributions of aerosol scattering from primary emissions plus carryover from the previous day and same-day secondary mechanisms, we will assume that Mexico City aerosol concentration and optics are due to primary sources that have concentrations determined mostly by diurnal variations in boundary layer dynamics and emission strengths, plus secondary sources that are affected both by boundary layer dynamics and photochemical transformations. Details of the myriad specific emission rates and secondary formation processes and their temporal variations are simplified into these two classes of aerosols. Denote by f_{sca} the fraction of scattering due to secondary as

$$f_{sca} = \frac{B_{sca}^{secondary}}{B_{sca}} = \frac{B_{sca} - \left(\frac{\omega_{prim}}{1-\omega_{prim}}\right) B_{abs}}{B_{sca}}. \quad (1)$$

In Eq. (1), ω_{prim} is the single scattering albedo associated with primary emissions. The numerical value of

$[\omega_{prim}/(1-\omega_{prim})]=1.16$ was determined by best fit of the f_{sca} curve to the f_{mass} curve discussed below. A value of $\omega_{prim}=0.54$ was found, commensurate with 75% of the primary aerosol extinction coming from compression ignition vehicle exhaust having a SSA of 0.4, and 25% of the primary aerosol extinction coming from sources like spark ignition vehicles and biomass combustion having a SSA of 0.95. The value of ω_{prim} is lower than the lowest value of the diurnally averaged SSA in Fig. 4 likely as a result that on the average, some aerosol carryover occurs from day to day. SSA values around ω_{prim} were observed in the morning hours following days with significant wind and rain that cleared out much of the background aerosol. The second term in Eq. (1) is a proxy for the primary emission of light scattering aerosol during all hours of the day. Equation (1) assumes that the sources of primary aerosol emissions that contribute most of the scattering and absorbing aerosols do not dramatically change on average during the course of the day. This assumption is likely to be valid during day light hours associated with the normal business workday since traffic related emissions dominate in Mexico City, and biomass burning impacts appear to have a similar diurnal cycle (Aiken et al., 2009). The quantity f_{sca} is further discussed below after a similar definition of the fraction of aerosol mass concentration due to secondary processes is developed.

The fractional aerosol mass due to photochemical production can also be estimated. Comparisons of the aerosol mass concentration with speciated data given in Fig. 6 are consistent with the secondary aerosol species (NH$_4$, NO$_3$, SO$_4$, and OOA interpreted as a surrogate for SOA) being photochemically produced and are hence correlated to the observed diurnal variations in precursor concentrations and solar radiation, with the exception of sulfate which is produced more regionally as described above. This interpretation is also consistent with previous studies (Salcedo et al., 2006; Volkamer et al., 2007). The total secondary aerosol mass concentration can be obtained from a sum of these species. The ratio, f_{mass}, of the sum of species having sunlight related diurnal variation to the total aerosol mass concentration is given in Eq. 2:

$$f_{mass} = \frac{OOA + NH_4 + NO_3 + SO_4}{OA + BC + IO}, \qquad (2)$$

where IO is the sum of all the inorganic species measured by the AMS as given in Fig. 6. Note that chloride has both primary and secondary sources in Mexico City (Salcedo et al., 2007; DeCarlo et al., 2007) and since its concentration is very small, it is not included in this calculation. This relationship is perhaps specific to Mexico City and may not be applicable to other locations having different geography and aerosol sources, but does give a measure of secondary aerosol production in a tropical megacity. The species in the numerator of Eq. (2) have a carryover from daylight hours and/or a regional background, so that f_{mass} would be non-zero even in nighttime hours.
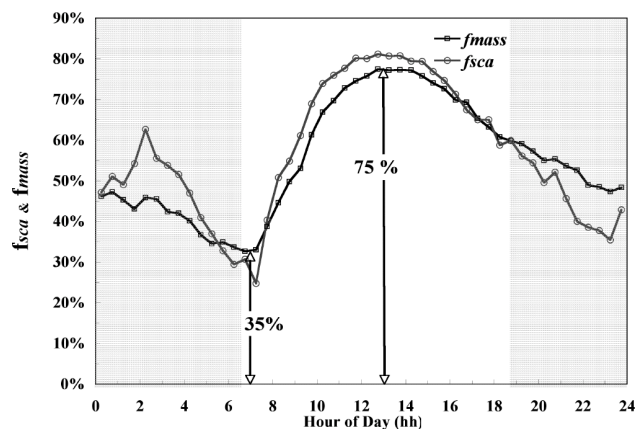

Fig. 10. Diurnal variation of the fraction of aerosol scattering and mass due to secondary photochemically related processes. The minimum occurs at sunrise due to relatively strong aerosol contributions by primary sources compared with carryover of secondary aerosol from the previous day. By noon, about 75% of the aerosol mass and scattering is due to secondary photochemically related production of aerosol.

The diurnal variation of the fraction of aerosol scattering and mass due to secondary photochemically related processes is shown in Fig. 10. The minimum of f_{sca} and f_{mass} is associated with secondary aerosol from regional background or carried over from the previous day. Some of the NH$_4$ is associated with SO$_4$ rather than NO$_3$. The aerosol fraction arising from secondary processes increases abruptly at sunrise, peaks at 11:00 a.m. to 02:00 p.m. and diminishes more gradually into the evening hours. The increase in the secondary contribution during daylight hours is inferred as the part of the curve for f_{mass} in the non-shaded region of Fig. 10. Around 75% of the aerosol scattering and mass is due to same-day secondary aerosol mass. While Fig. 10 is a rough approximation and in particular ignores the impact of crustal species, an estimate of the relative fraction of secondary aerosol impacts is useful to help frame the problem for the modeling community.

Figure 11 shows the diurnal variations of aerosol light absorption measured with the photoacoustic instrument and the aethalometer along with the percentage difference of these values, with the photoacoustic values in the denominator. The aethalometer values are around 15% lower than PAS values from 03:00 a.m. until 06:00 a.m., consistent with a reduction of the multiple scattering enhancement factor of the aethalometer filter media during the time of the lowest SSA (Arnott et al., 2005) . The percentage difference between PAS and aethalometer instruments has a daily variation of about 25% in total (from a maximum of about +15% to a minimum of about −10%). The OOA diurnal variation is also displayed as an indicator of time when secondary organic aerosol concentration is highest. The aethalometer data is about 10% greater than photoacoustic values from 10:00 a.m. to 01:00 p.m. coincident with the peak OOA and
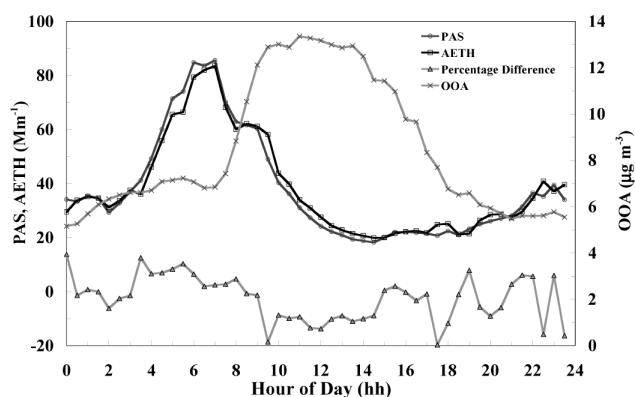
Fig. 11. Percentage difference between PAS and aethalometer instruments as a function of time of day, and the OOA.

SSA. This is in contrast to the report by Lack et al. (2008) of a strong positive bias of greater than 40% for a filter based measurement of aerosol light absorption by the particle soot absorption photometer (PSAP) compared with photoacoustic values when OOA concentration was high in Houston, Texas, USA. The difference in the present work and that reported by Lack may be due to aerosol composition differences and/or PSAP and aethalometer filter media differences (Arnott et al., 2005).

4 Conclusions

Peak absorption in Mexico City occurs early in the morning before boundary layer expansion. Aerosol scattering peaks several hours later than absorption, and photochemically produced aerosol mass is likely the cause of this increase in aerosol light scattering at the Mexico City urban site. Peak scattering occurs as a balance between photochemical production and aerosol dilution as the atmospheric boundary layer extends to larger heights during daylight hours, and average wind speeds increase. Aerosol SSA has a minimum value of 0.60 in the early morning hours as the rush hour traffic is most intense and dilution is limited in a shallow boundary layer. For comparison, the SSA for diesel soot alone would be anticipated to be 0.4 at 532 nm (Sheridan et al., 2005). Values at night are somewhat greater than in the early morning hours, indicating that on average there is some carryover from the previous day to the next. As well, other aerosol sources such as cooking and spark ignition vehicle traffic may contribute to the observed SSA variance. The strong diurnal behavior of the SSA clearly shows that secondary aerosol formation from photochemical processes in Mexico City begins to affect the aerosol radiative forcing values as soon as the sun rises, which is consistent with the strong secondary source observed in previous studies (Salcedo et al., 2006; Volkamer et al., 2006). The SSA values increase at the MCMA site until about 11:00 a.m. when the atmospheric boundary layer height increases and dilutes the accumulated primary and secondary aerosol. At this time, 75% of the scattering and aerosol mass is due to sameday secondary aerosol production during daylight hours. A 10% systematic bias was detected for filter-based measurement of aerosol light absorption in the presence of substantial secondary organic aerosol mass concentration and peak SSA. The average diurnal range of single scattering albedo and secondary aerosol mass and scattering coefficient provide a reasonable estimate of the range of radiative values for aerosols being produced and transported from a tropical megacity. Further work will be needed to make use of this data and other MILAGRO data sets in conjunction with atmospheric models to refine the variability important for assessment of the impact of aerosols on radiative forcing as well as photochemical production of oxidants and secondary aerosols relevant to air quality issues.

References

Aiken, A. C., DeCarlo, P. F., Kroll, J. H., Worsnop, D. R., Huffman, J. A., Docherty, K., Ulbrich, I. M., Mohr, C., Kimmel, J. R., Sueper, D., Zhang, Q., Sun, Y., Trimborn, A., Northway, M., Ziemann, P. J., Canagaratna, M. R., Onasch, T. B., Alfarra, R., Prevot, A. S. H., Dommen, J., Duplissy, J., Metzger, A., Baltensperger, U., and Jimenez, J. L.: O/C and OM/OC Ratios of Primary, Secondary, and Ambient Organic Aerosols with High Resolution Time-of-Flight Aerosol Mass Spectrometry, Environ. Sci. Technol., 42, 4478–4485, 2008.

Aiken, A. C., Salcedo, D., Cubison, M. J., de Foy, B., Wiedinmyer, C., Huffman, A., DeCarlo, P. F., Ulbrich, I., Docherty, K., Sueper, D., Kimmel, J. R., Worsnop, D., Trimborn, A., Northway, M., Wehrli, M. N., Szidat, S., Prevot, A. S. H., Baltensperger, U., Noda, J., Wacker, L., Stone, E. A., Schauer, J. J., Volkamer, R., Fortner, E., Knighton, B., Wang, J., Laskin, A., Zheng, J., Zhang, R., Gaffney, J., Marley, N. A., Querol, X., Paredes-Miranda, G., Arnott, W. P., Molina, L. T., Sosa, G., and Jimenez, J. L.: Mexico City Aerosol Analysis during MILAGRO using High Resolution Aerosol Mass Spectrometry at the Urban Supersite (T0). Part 1: Overall Fine Particle Composition and

Organic Source Apportionment., Atmos. Chem. Phys. Discuss., 9, 8377–8427, 2009, http://www.atmos-chem-phys-discuss.net/9/8377/2009/.

Anderson, T. L., Covert, D. S., Marshall, S. F., Laucks, M. L., Charlson, R. J., Waggoner, A. P., Ogren, J. A., Caldow, R., Holm, R. L., Quant, F. R., Sem, G. J., Wiedensohler, A., Ahlquist, N. A., and Bates, T. S.: Performance characteristics of a high sensitivity, three wavelength, total scatter/backscatter nephelometer, Journal of Atmospheric and Oceanic Technology, 13, 967–986, 1996.

Andreae, M. O.: The dark side of aerosols, Nature, 409, 671–672, 2001.

Andreae, M. O. and Gelencsér, A.: Black carbon or brown carbon? The nature of light-absorbing carbonaceous aerosols, Atmos. Chem. Phys., 6, 3131–3148, 2006, http://www.atmos-chem-phys.net/6/3131/2006/.

Arnott, W. P., Hamasha, K., Moosmüller, H., Sheridan, P. J., and Ogren, J. A.: Towards aerosol light absorption measurements with a 7-wavelength Aethalometer: Evaluation with a photoacoustic instrument and a 3 wavelength nephelometer, Aerosol Sci. Tech., 39, 17–29, 2005.

Arnott, W. P., Moosmüller, H., Rogers, C. F., Jin, T., and Bruch, R.: Photoacoustic spectrometer for measuring light absorption by aerosols: Instrument description, Atmos. Environ., 33, 2845–2852, 1999.

Arnott, W. P., Moosmüller, H., and Walker, J. W.: Nitrogen dioxide and kerosene-flame soot calibration of photoacoustic instruments for measurement of light absorption by aerosols., Rev. Sci. Inst., 71(7), 4545–4552, 2000.

Bergin, M. H., Cass, G. R., Xu, J., Fang, C., Zeng, L. M., Yu, T., Salmon, L. G., Kiang, C. S., Tang, X. Y., Zhang, Y. H., and Chameides, W. L.: Aerosol radiative, physical, and chemical properties in Beijing during June 1999, J. Geophys. Res., 106(D16), 17969–17980, 2001.

Bond, T. C., Anderson, T. L., and Campbell, D.: Calibration and Intercomparison of Filter-Based Measurements of Visible Light Absorption by Aerosols, Aerosol Sci. Tech., 30(6), 582–600, 1999.

Bond, T. C. and Bergstrom, R. W.: Light absorption by carbonaceous particles: An investigative review., Aerosol Sci. Tech., 40, 27–67, 2006.

Canagaratna, M. R., Jayne, J. T., Jimenez, J. L., Allan, J. D., Alfarra, M. R., Zhang, Q., Onasch, T. B., Drewnick, F., Coe, H., Middlebrook, A., Delia, A., Williams, L. R., Trimborn, A. M., Northway, M. J., DeCarlo, P. F., Kolb, C. E., Davidovits, P., and Worsnop, D. R.: Chemical and Microphysical Characterization of Ambient Aerosols with the Aerodyne Aerosol Mass Spectrometer, Mass Spectrom. Rev., 26, 185–222, 2007.

Charlson, R. J., Schwartz, S. E., Hales, J. M., Cess, R. D., Coakley, J. A., Hansen, J. E., and Hofmann, D. J.: Climate Forcing by Anthropogenic Aerosols, Science, 255, 423–429, 1992.

de Almeida Castanho, A., Prinn, R., Martins, V., Herold, M., Ichoku, C., and Molina, L.: Analysis of Visible/SWIR surface reflectance ratios for aerosol retrievals from satellite in Mexico City urban area., Atmos. Chem. Phys., 7, 5467–5477, 2007, http://www.atmos-chem-phys.net/7/5467/2007/.

de Foy, B., Varela, J. R., Molinta, L. T., and Molina, M. J.: Rapid ventilation of the Mexico City basin and regional fate of the urban plume, Atmos. Chem. Phys., 6, 2321–2335, 2006, http://www.atmos-chem-phys.net/6/2321/2006/.

DeCarlo, P. F., Dunlea, E. J., Kimmel, J. R., Aiken, A. C., Sueper, D., Crounse, J., Wennberg, P. O., Emmons, L., Shinozuka, Y., Clarke, A., Zhou, J., Tomlinson, J., Collins, D. R., Knapp, D., Weinheimer, A. J., Montzka, D. D., Campos, T., and Jimenez, J. L.: Fast Airborne Aerosol Size and Chemistry Measurements with the High Resolution Aerosol Mass Spectrometer during the MILAGRO Campaign, Atmos. Chem. Phys., 8, 4027–4048, 2008, http://www.atmos-chem-phys.net/8/4027/2008/.

DeCarlo, P. F., Kimmel, J. R., Trimborn, A., Northway, M. J., Jayne, J. T., Aiken, A. C., Gonin, M., Fuhrer, K., Horvath, T., Docherty, K., Worsnop, D. R., and Jimenez., J. L.: Field-Deployable, High-Resolution, Time-of-Flight Aerosol Mass Spectrometer, Anal. Chem., 78, 8281–8289, 2006.

Haywood, J. M. and Ramaswamy, V.: Global sensitivity studies of the direct radiative forcing due to anthropogenic sulfate and black carbon aerosols, J. Geophys. Res., 103(D6), 6043–6058, 1998.

Herndon, S. C., Onasch, T. B., Wood, E. C., Kroll, J. H., Canagaratna, M. R., Jayne, J. T., Zavala, M. J. A., Knighton, W. B., Mazzoleni, C., Dubey, M. K., Ulbrich, I. M., Jimenez, J. L., Seila, R., de Gow, J. A., de Foy, B., Fast, J. D., Molina, L. T., Kolb, C. E., and Worsnop, D.: Correlation of secondary organic aerosol with odd oxygen in Mexico City, Geophys. Res. Lett., 35, L15804, doi:10.1029/2008GL034058, 2008.

Huffman, J., Jayne, J., Drewnick, F., Aiken, A., Onasch, T., Worsnop, D., and Jimenez, J.: Design, Modeling, Optimization, and Experimental Tests of a Particle Beam Width Probe for the Aerodyne Aerosol Mass Spectrometer, Aerosol Sci. Tech., 39(12), 21, 2005.

Jacobson, M. Z.: Strong Radiative Heating due to the Mixing State of Black Carbon in Atmospheric Aerosols, Nature, 409, 695–697, 2001.

Jauregui, E. and Luyando, E.: Global radiation attenuation by air pollution and its effects on the thermal climate in Mexico City, Int. J. Climatol., 19(6), 683–694, 1999.

Jimenez, J. L., Bahreini, R., Cocker, D. R., Zhuang, H., Varutbangkul, V., Flagan, R. C., Seinfeld, J. H., O'Dowd, C. and Hoffmann, T.: New Particle Formation from Photooxidation of Diiodomethane (CH2I2), J. Geophys. Res.-Atmos., 108, (D10), 4318, doi:10.1029/2002JD002452, 2003.

Johnson, K. S., Zuberi, B., Molina, L. T., Molina, M. J., Iedema, M. J., Cowin, J. P., Gaspar, D. J., Wang, C., and Laskin, A.: Processing of soot in an urban environment: case study from the Mexico City Metropolitan Area, Atmos. Chem. Phys., 5, 3033–3043, 2005, http://www.atmos-chem-phys.net/5/3033/2005/.

Kirchstetter, T. W., Novakov, T., and Hobbs, P. V.: Evidence that the spectral dependence of light absorption by aerosols is affected by organic carbon, J. Geophys. Res., 109, D21208, doi:10.1029/2004JD00499, 2004.

Lack, D. A., Cappa, C. D., Covert, D. S., Baynard, T., Massoli, P., Sierau, B., Bates, T. S., Quinn, P. K., Lovejoy, E. R., and Ravishankara, A. R.: Bias in Filter Based Aerosol Absorption Measurements Due to Organic Aerosol Loading: Evidence from Ambient Measurements, Aerosol Sci. Tech., 42(12), 1033–1041, 2008.

Lewis, K., Arnott, W. P., Moosmüller, H., and Wold, C. E.: Strong spectral variation of biomass smoke light absorption and single scattering albedo observed with a novel dual wavelength

photoacoustic instrument, J. Geophys. Res., 113, D16203, doi:10.1029/2007JD009699, 2008.

Mar, E., Sheinbaum, N. A., and Luna, N.: Inventario de emisiones y posibles politicas de mitigacion de gases contaminantes provenientes del sector transporte del area metropolitana de la ciudad de Mexico, Preceedings, Contaminacion Atmosferica III, Instituto de Geofisica, UNAM, 313–339, 2001.

Mayol-Bracero, O. L., Gabriel, R., Andreae, M. O., Kirchsteter, T. W., Novakov, T., Ogren, J., Sheridan, P., and Streets, D. G.: Carbonaceous aerosols over the Indian Ocean during the Indian Ocean Experiment (INDOEX): Chemical characterization, optical properties, and probable sources, J. Geophys. Res., 107(D19), 8030, doi:10.1029/2000JD0039, 2002.

McComiskey, A., Schwartz, S. E., Schmid, B., Guan, H., Lewis, E. R., Ricchiazzi, P., and Ogren, J. A.: Direct aerosol forcing: Calculation from observables and sensitivities to inputs, J. Geophys. Res., 113, D09202, doi:10.1029/2007JD009170, 2008.

Molina, L. T., Kolb, C. E., de Foy, B., Lamb, B. K., Brune, W. H., Jimenez, J. L., Ramos- Villegas, R., Sarmiento, J., Paramo-Figueroa, V. H., Cardenas, B., Gutierrez-Avedoy, V., and Molina, M. J.: Air Quality in North America's Most Populous City – Overview of the MCMA-2003 Campaign., Atmos. Chem. Phys., 7, 2447–2473, 2007,
http://www.atmos-chem-phys.net/7/2447/2007/.

Paatero, P. and Tapper, U.: Positive matrix factorization: A nonnegative factor model with optimal utilization of error estimates of data values, Environmetrics, 5, 111–126, 1994.

Querol, X., Pey, J., Minguillon, M. C., Perez, N., Alastuey, A., Viana, M., Moreno, T., Bernabe, R. M., Blanco, S., Cardenas, B., Vega, E., Sosa, G., Escalona, S., Ruiz, H., and Artinano, B.: PM speciation and sources in Mexico during MILAGRO campaign, Atmos. Chem. Phys., 8, 111–128, 2008,
http://www.atmos-chem-phys.net/8/111/2008/.

Rahmah, A. A., Arnott, W. P., and Moosmüller, H.: Integrating nephelometer with a low truncation angle and an extended calibration scheme, Measurement Sci. Technol., 17, 1723–1732, 2006.

Salcedo, D., Onasch, T. B., Canagaratha, M., Dzepina, K., Huffman, J. A., Jayne, J. T., Worsnop, D., Kolb, C., Weimer, S., Drewnick, F., Allan, J., A., D. and Jimenez, J.: Technical Note: Use of a beam width probe in an Aerosol Mass Spectrometer to monitor particle collection efficiency in the field., Atmos. Chem. Phys., 7, 549–556, 2007,
http://www.atmos-chem-phys.net/7/549/2007/.

Salcedo, D., Onasch, T. B., Dzepina, K., Canagaratna, M. R., Zhang, Q., Huffman, J. A., DeCarlo, P. F., Jayne, J. T., Mortimer, P., Worsnop, D. R., Kolb, C. E., Johnson, K. S., Zuberi, B., Marr, L. C., Volkamer, R., Molina, L. T., Molina, M. J., Cardenas, B., Bernabe, R. M., Marquez, C., Gaffney, J. S., Marley, N. A., Laskin, A., Shutthanandan, V., Xie, Y., Brune, W., Lesher, R., Shirley, T., and Jimenez, J. L.: Characterization of ambient aerosols in Mexico City during the MCMA-2003 campaign with Aerosol Mass Spectrometry: results from the CENICA Supersite, Atmos. Chem. Phys., 6, 925–946, 2006,
http://www.atmos-chem-phys.net/6/925/2006/.

Sheridan, P. J., Arnott, W. P., Ogren, J. A., Anderson, B. E., Atkinson, D. B., Covert, D. S., Moosmuller, H., Petzold, A., Schmid, B., Strawa, A. W., Varma, R., and Virkkula, A.: The Reno aerosol optics study: An Evaluation of Aerosol Absorption Mea-

surement Methods, Aerosol Sci. Tech., 39, 1–16, 2005.

Stone, E. A., Snyder, D. C., Sheesley, R. J., Sullivan, A. P., Weber, R. J., and Schauer, J. J.: Source apportionment of fine organic aerosol in Mexico City during the MILAGRO experiment 2006, Atmos. Chem. Phys., 8, 1249–1259, 2008,
http://www.atmos-chem-phys.net/8/1249/2008/.

Subramanian, R., Roden, C. A., Boparai, P., and Bond, T. C.: Yellow beads and missing particles: Trouble ahead for filter-based absorption measurements., Aerosol Sci. Tech., 41, 630–637, 2007.

Sun, H., Biedermann, L., and Bond, T. C.: Color of brown carbon: A model for ultraviolet and visible light absorption by organic carbon aerosol, Geophys. Res. Lett., 34, L17813, doi:10.1029/2007GL029797, 2007.

Ulbrich, I. M., Canagaratna, M. R., Zhang, Q., Worsnop, D. R. and Jimenez, J. L.: Interpretation of Organic Components from Positive Matrix Factorization of Aerosol Mass Spectrometric Data, Atmos. Chem. Phys. Discuss., 8, 6729–6791, 2008,
http://www.atmos-chem-phys-discuss.net/8/6729/2008/.

Virkkula, A., Mäkelä, T., Hillamo, R., Yli-Tuomi, T., Hirsikko, A., Hämeri, K., and Koponen, I. K.: A simple procedure for correcting loading effects of aethalometer data, J. Air Waste Manage., 57, 1214–1222, 2007.

Volkamer, R., Jimenez, J. L., Martini, F. S., Dzepina, K., Zhang, Q., Salcedo, D., Molina, L. T., Worsnop, D. R., and Molina, M. J.: Secondary organic aerosol formation from anthropogenic air pollution: Rapid and higher than expected, Geophys. Res. Lett., 33, L178111, doi:10.1029/2006GL026899, 2006.

Volkamer, R., Martini, F. S., Molina, L. T., Salcedo, D., Jimenez, J. L., and Molina, M. J.: A missing sink for gas-phase glyoxal in Mexico City: Formation of secondary organic aerosol, Geophys. Res. Lett., 34, L19807, doi:10.1029/2007GL030752, 2007.

Weingartner, E., Saathoff, H., Schnaiter, M., Streit, N., Bitnar, B., and Baltensperger, U.: Absorption of light by soot particles: determination of the absorption coefficient by means of aethalometers, J. Aerosol Sci., 34, 1445–1463, 2003.

Yokelson, R. J., Urbanski, S. P., Atlas, E. L., Toohey, D. W., Alvarado, E. C., Crounse, J. D., Wennberg, P. O., Fisher, M. E., Wold, C. E., Campos, T. L., Adachi, K., Buseck, P. R., and Hao, W. M.: Emissions from Forest Fires near Mexico City, Atmos. Chem. Phys., 7, 5569–5584, 2007,
http://www.atmos-chem-phys.net/7/5569/2007/.

Zhang, Q., Jimenez, J. L., Canagaratna, M. R., Allan, J. D., Coe, H., Ulbrich, I., Alfarra, M. R., Takami, A., Middlebrook, A. M., Sun, Y. L., Dzepina, K., Dunlea, E., Docherty, K., DeCarlo, P. F., Salcedo, D., Onasch, T., Jayne, J. T., Miyoshi, T., Shimono, A., Hatakeyama, S., Takegawa, N., Kondo, Y., Schneider, J., Drewnick, F., Borrmann, S., Weimer, S., Demerjian, K., Williams, P., Bower, K., Bahreini, R., Cottrell, L., Griffin, R. J., Rautiainen, J., Sun, J. Y., Zhang, Y. M., and Worsnop, D. R.: Ubiquity and Dominance of Oxygenated Species in Organic Aerosols in Anthropogenically-Influenced Northern Hemisphere Mid-latitudes, Geophys. Res. Lett., 34, L13801, doi:10.1029/2007GL029979, 2007.

Zhang, Q., Worsnop, D. R., Canagaratna, M. R., and Jimenez, J. L.: Hydrocarbon-like and oxygenated organic aerosols in Pittsburgh: Insights into sources and processes of organic aerosols, Atmos. Chem. Phys., 5, 3289–3311, 2005,
http://www.atmos-chem-phys.net/5/3289/2005/.